Draft version April 27, 2020
Typeset using LaTeX default style in AASTeX62

Milestone III: Integrating the initial perturbations.

Håkon Tansem

1. INTRODUCTION

This is the third milestone in a four milestone project where the end goal is to compute the CMB power spectrum. In the previous two milestones we have solved for the background evolution of the universe Tansem (2020a) as well as studying the recombination history of the universe Tansem (2020b). In this third milestone we will study how perturbations has evolved throughout cosmic history. We will start with the initial conditions as predicted by inflation and solve the Boltzmann and and Einsteins equations for baryons, cold dark matter and photons as well as the metric perturbations.

2. METHOD

In this model we assume a few simplifications. We neglect photon polarization and ignore neutrinos as to reduce the number of equations. We will therefore only study the evolution of the density parameter δ and velocity parameter v for baryons and dark matter, the perturbation to the photon distribution θ_ℓ, where we include integer multipoles $\ell \in [0, 7]$, as well as the metric perturbations Φ and Ψ all as functions of $x = log(a)$. When studying the perturbations we will work in fourier space where each mode is denoted by the magnitude of its wavevector k. When integrating the perturbations we have two main regimes to take into account. In early times, as we calculated in milestone II, we saw that the optical depth of the universe $\tau \gg 1$ due to all electrons being free. This means that at any given point in space the mean free path for a photon is very small. This gives very little anisotropy as only perturbations very close by can be observed. This suppresses all higher multipoles and washes out their gradients making only $\ell = 0$ and $\ell = 1$ the nonnegligible moments. This makes photons behave like a fluid described by the two variables density and velocity which in our case is represented by θ_0 and θ_1 respectively (Dodelson 2003, p. 225). As criterions for deciding wether we are in the tight coupling regime we check wether we are past the onset of recombination, at which time we approximate by evualuating the free electron fraction X_e and seeing wether it is smaller than 0.99, or if the criterion $\left|\frac{d\tau}{dx}\right| < 10 \cdot \min(1, \frac{ck}{\mathcal{H}})$ is met. That is if $X_e < 0.99$ or if the criterion is met, we assume that we are no longer in the tight coupling regime.

When solving the equations we start by setting the initial conditions given by inflation as

$$\Psi = -\frac{2}{3} \tag{1}$$

$$\Phi = -\Psi \tag{2}$$

$$\delta_{\text{CDM}} = \delta_b = -\frac{3}{2}\Psi \tag{3}$$

$$v_{\text{CDM}} = v_b = -\frac{ck}{2\mathcal{H}}\Psi \tag{4}$$

$$\Theta_0 = -\frac{1}{2}\Psi \tag{5}$$

$$\Theta_1 = +\frac{ck}{6\mathcal{H}}\Psi \tag{6}$$

$$\Theta_2 = -\frac{20ck}{45\mathcal{H}\tau'}\Theta_1, \tag{7}$$

$$\Theta_\ell = -\frac{\ell}{2\ell+1}\frac{ck}{\mathcal{H}\tau'}\Theta_{\ell-1}. \tag{8}$$

$$\tag{9}$$

All equations in this paper are given by Winther (2020) unless otherwise stated. The full set of ODE's for the photon multipoles are given as

$$\Theta_0' = -\frac{ck}{\mathcal{H}}\Theta_1 - \Phi', \tag{10}$$

$$\Theta_1' = \frac{ck}{3\mathcal{H}}\Theta_0 - \frac{2ck}{3\mathcal{H}}\Theta_2 + \frac{ck}{3\mathcal{H}}\Psi + \tau'\left[\Theta_1 + \frac{1}{3}v_b\right], \tag{11}$$

$$\Theta_\ell' = \frac{\ell ck}{(2\ell+1)\mathcal{H}}\Theta_{\ell-1} - \frac{(\ell+1)ck}{(2\ell+1)\mathcal{H}}\Theta_{\ell+1} + \tau'\left[\Theta_\ell - \frac{1}{10}\theta_2\delta_{\ell,2}\right], \qquad 2 \le \ell < \ell_{\max} \tag{12}$$

$$\Theta_\ell' = \frac{ck}{\mathcal{H}}\Theta_{\ell-1} - c\frac{\ell+1}{\mathcal{H}\eta(x)}\Theta_\ell + \tau'\Theta_\ell, \qquad \ell = \ell_{\max}. \tag{13}$$

$$\tag{14}$$

where $\delta_{\ell,2}$ is the kroenecker-delta and $\eta(x)$ is the conformal time computed in milestone I. For cold dark matter and baryons as well as the metric perturbations, we have

$$\delta_{\rm CDM}' = \frac{ck}{\mathcal{H}}v_{\rm CDM} - 3\Phi' \tag{15}$$

$$v_{\rm CDM}' = -v_{\rm CDM} - \frac{ck}{\mathcal{H}}\Psi \tag{16}$$

$$\delta_b' = \frac{ck}{\mathcal{H}}v_b - 3\Phi' \tag{17}$$

$$v_b' = -v_b - \frac{ck}{\mathcal{H}}\Psi + \tau' R(3\Theta_1 + v_b) \tag{18}$$

$$\Phi' = \Psi - \frac{c^2k^2}{3\mathcal{H}^2}\Phi + \frac{H_0^2}{2\mathcal{H}^2}\left[\Omega_{\rm CDM}e^{-x}\delta_{\rm CDM} + \Omega_{b,0}e^{-x}\delta_b + 4\Omega_{r,0}a^{-2}\Theta_0\right] \tag{19}$$

$$\Psi = -\Phi - \frac{12H_0^2}{c^2k^2e^{2x}}\Omega_{r,0}\Theta_2, \tag{20}$$

$$\tag{21}$$

where $R = \frac{4\Omega_{r,O}}{3\Omega_{b,0}e^x}$. These equations apply as they are written when we have exited the tight coupling regime. In the tight coupling regime, as described earlier, multipoles larger than $\ell = 1$ have their gradients washed out. This gives the following changes to the set of equations

$$q = \frac{-[(1-R)\tau' + (1+R)\tau'](3\Theta_1 + v_b) - \frac{ck}{\mathcal{H}}\Psi + (1 - \frac{\mathcal{H}'}{\mathcal{H}})\frac{ck}{\mathcal{H}}(-\Theta_0 + 2\Theta_2) - \frac{ck}{\mathcal{H}}\Theta_0'}{(1+R)\tau' + \frac{\mathcal{H}'}{\mathcal{H}} - 1} \tag{22}$$

$$v_b' = \frac{1}{1+R}\left[-v_b - \frac{ck}{\mathcal{H}}\Psi + R(q + \frac{ck}{\mathcal{H}}(-\Theta_0 + 2\Theta_2) - \frac{ck}{\mathcal{H}}\Psi)\right] \tag{23}$$

$$\Theta_1' = \frac{1}{3}(q - v_b'). \tag{24}$$

Note that Θ_0' is still the same as given by equation 10. In the tight coupling regime the higher order multipoles are given by their initial values as shown in equations 7 and 8. The differential equations given are solved numerically for every fourier mode k given in a logarithmically spaced intervall between $k_{min} = 0.00005$ and $k_{max} = 0.3$. Each fourier mode is solved on a linearly spaced $x-$interval ranging from $x_{min} = log(1e-8)$ to present time at $x_{max} = 0$. The solution for each fourier mode for all of the components are stored so that they can ble splined. This gives us the ability to evaluate each component for an arbitrary x and k value.

3. RESULTS

All results were produced using a cosmology with $\Omega_{b,0} = 0.05$, $\Omega_{cdm,0} = 0.25$, $\Omega_{\Lambda,0} = 0.7$ and $h = 0.7$. From using data from milestone I matter-radiation equality a_{eq} was calculated to correspond to $x = -8.68$ which will be used in most results as a reference point. To illustrate three different regimes relative to horizon entry three fourier modes $k = 0.001$, $k = 0.05$ and $k = 0.3$ were chosen to present the main results.

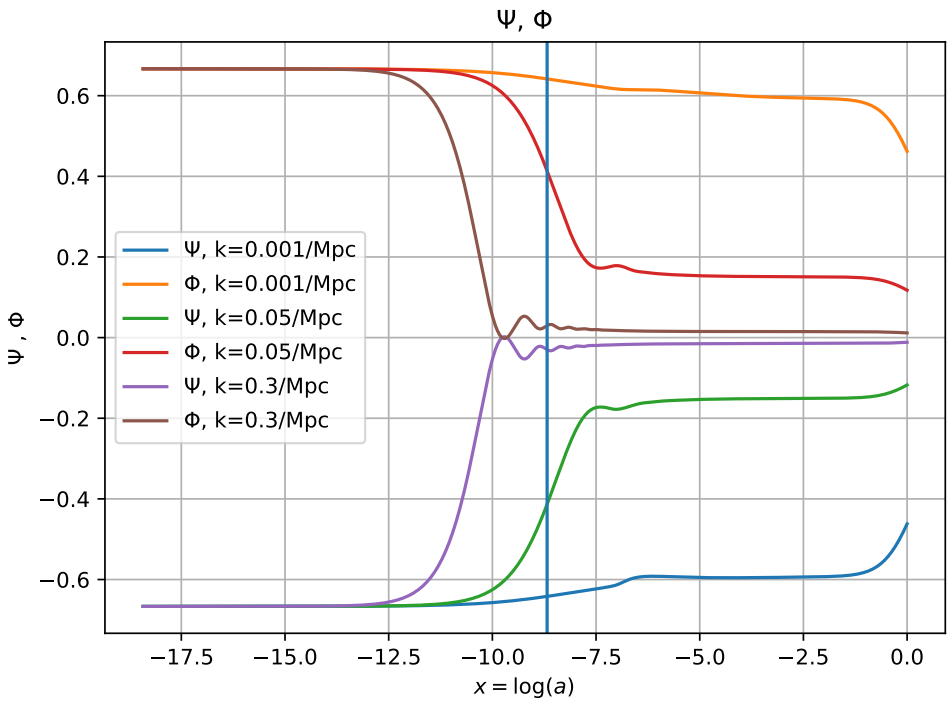

Figure 1. Figure showing the Metric perturbations Ψ and Φ as functions of $x = log(a)$ for three different fourier modes k. The time a_{eq} is plotted as a straight line

When solving the equations for the metric perturbations Φ and Ψ for the different fouries modes k, our model produced the results shown in figure 1. Further we have the solutions for the density and velocity parameters for baryons and cold dark matter for the three different fourier modes illustrated in figures 2 and 3 respectively. The results for the monopole θ_0 and multipole θ_1 is presented in figure 4 and figure 5. As a means to compare the monopole and δ_b parameter, they were both plotted in figure 6 for a fourier mode $k = 0.1$. Here the first two maximas of the monopole is plotted as vertical lines to illustrate overlap with fluctuations in δ_b.

4. DISCUSSION

When studying the result for the metric perturbations Φ and Ψ, as shown in figure 1, one can clearly see that horizon entry for the different scales has a significant impact on the behavior. Due to the second term in equation 20 being much smaller than Φ we have approximately that $\Phi = -\Psi$. When looking at Φ, which represents the gravitational potential, one can see that the smaller the scale, the earlier it enters the horizon and starts to decrease. One noticeable difference is horizon entry relative to a_{eq}. During the radiation dominated era matter wont cluster easily. This can be a contributor to the potential decreasing. If matter wont cluster as easily at the same time as the universe expands then the potential will decay. The smallest mode decays to zero while the second largest mode $k = 0.05$ enters in the radiation dominated era, but before it decays to zero, the universe enters matter domination. In the matter dominated era the evolution of the potential is frozen out (Baumann 2020, p.104). The largest scale which only enters late into the matter dominated era still experiences a change of a factor $\frac{9}{10}$ during the transition from radiation to matter domination which is given by the transfer function (Dodelson 2003, p.182). The monopole θ_0 and dipole θ_1 is shown in figures 4 and 5 respectively. For the smallest scale which enters the horizon first inside the tight coupling regime, one can see that the monopole starts to increase. Now that the mode has entered the horizon, gravity begins to act causing the density and photon temperature to increase. This will in turn cause the pressure to increase and the solution will fluctuate. After recombination the largest mode freezes out. The second largest mode $k = 0.5$ experiences the same behaviour for both the monopole and the multipole before it turns into a chaotic behaviour after recombination. The largest mode enters the horizon well after recombination and is not easily described by the fluid analogy as in the tight coupling regime.

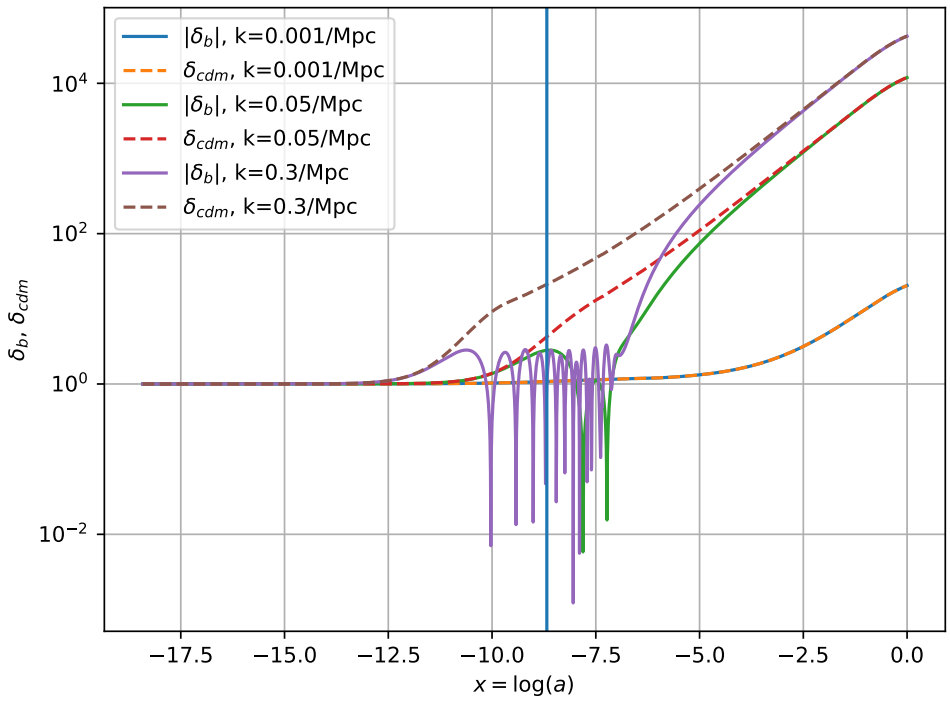

Figure 2. Figure showing the δ parameter for baryons and cold dark matter as functions of x for three different fourier modes k. The time a_{eq} is plotted as a straight line

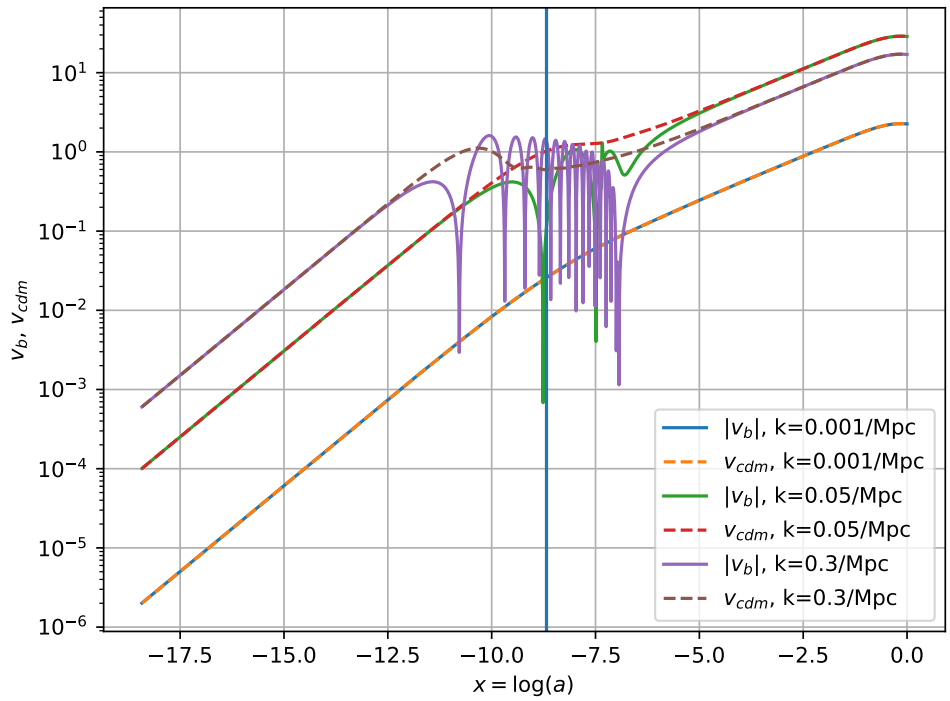

Figure 3. Figure showing the v parameter for baryons and cold dark matter as functions of x for three fourier different modes k. The time a_{eq} is plotted as a straight line

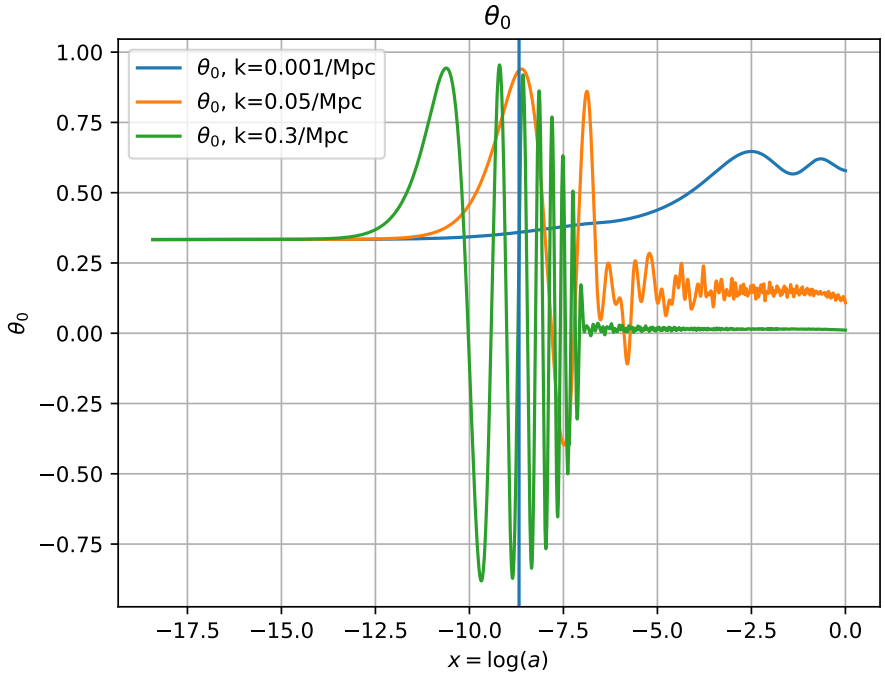

Figure 4. Figure showing the monopole θ_0 functions of x for three different fourier modes k. The time a_{eq} is plotted as a straight line

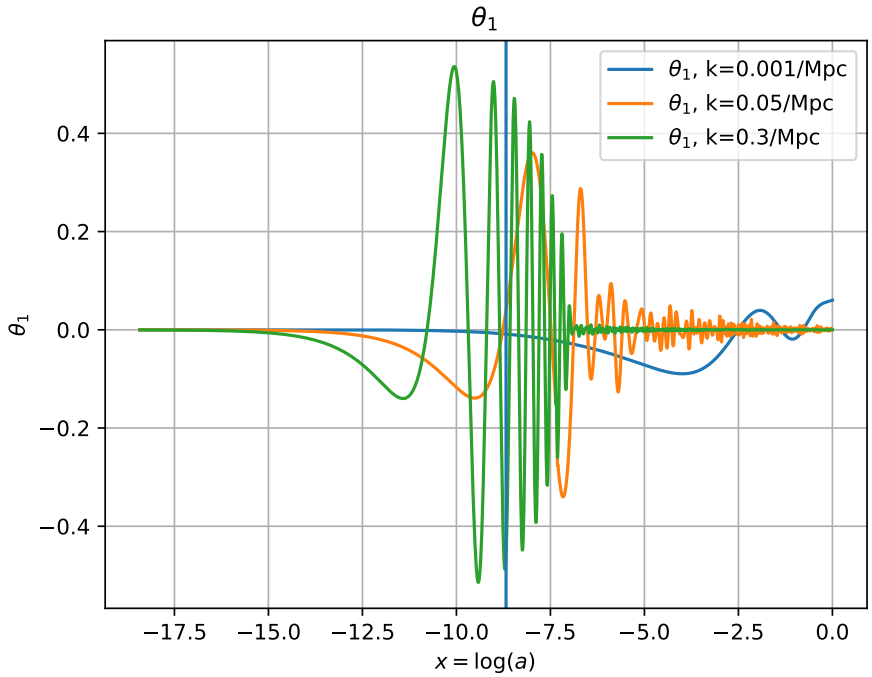

Figure 5. Figure showing the multipole θ_1 functions of x for three different fourier modes k. The time a_{eq} is plotted as a straight line

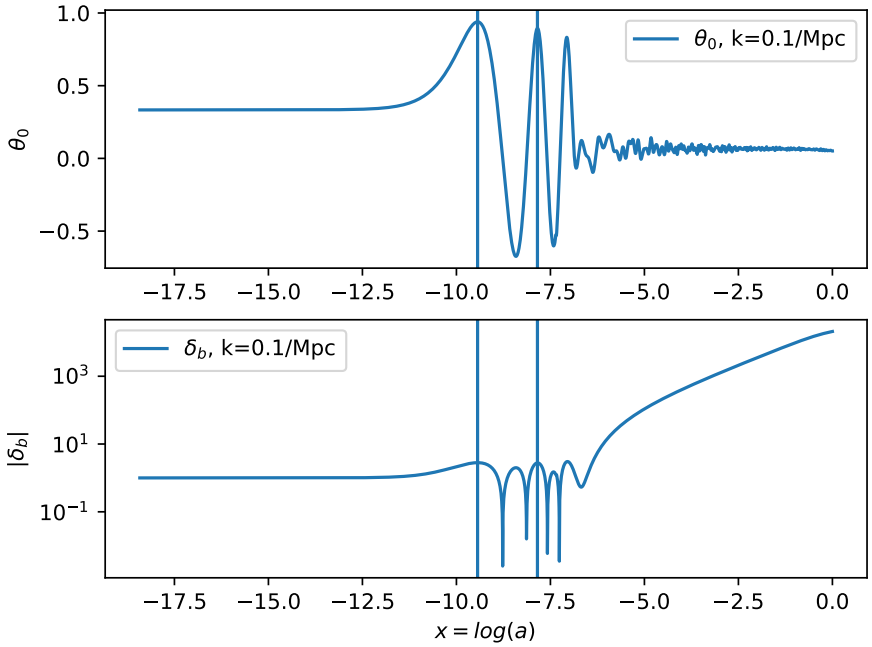

Figure 6. Figure showing the monopole monopole θ_0 as well as the density parameter for baryons δ_b for a fourier mode that completes a few oscillations before recombination. The first two maximas of the monopole is plottet as straight lines to illustrate overlap with maximas in the baryon density fluctuations.

The evolution of the density parameter, illustrated in figure 2, Shows clear differences on the different scales. One can see that the density starts to increase for the smaller scales first as they enter the horizon. Another interesting feature is the change of gradient as the universe transitions from radiation to matter domination. For $k = 0.3$ one can see that it enters the horizon well inside the radiation dominated era with a steep slope. As we transition from radiation to matter domination the slope gets gradually smaller untill we get a constant slope again when we have full matter domination. From milestone I, we saw that this transition happened over an extended period of time which is also reflected in this plot. For the largest scales that enter well after a_{eq}, when the universe is fully matter dominated, we see that the density starts to increase with a similar slope as the smaller scales has in the matter dominated era. By looking at the evolution of the velocity paramter, as shown in figure 3, one can see that the velocity is relatively small, but grows to the order of 10^0 as they enter the horizon. Just as for the density parameter the different regimes are evident in the slopes of the velocity for the different modes. One interesting feature is fluctuations in the baryonic density and baryon velocity while the same components for cold dark matter experiences a smooth evolution. The cause for this is the fact that baryons experience pressure while cold dark matter does not. Figure 6 shows the evolution of the monopole and the baryon density for $k = 0.1$. The location of the first two peaks of the monopole fluctuation is plotted for both parameters. Here we can clearly see that the baryonic density fluctuates in phase with the monopole during the tight coupling regime. The baryonic density is then suppressed untill it starts to increase again when the monopole freezes out during the matter dominated era. The fact that dark matter is pressureless is important for structure formation in the universe. Since the dark matter is not suppressed it will continue to evolve and create potential wells that baryonic matter later can fall into and is an essential requirement for the structure we see in the universe today (Shen 2019, p.15).

We have created a model for integrating and solving the perturbations given by the Einstein and Boltzmann equations. Allthough we have neglected polarization and neutrinos our results still provide solution that can be explained by known physics and are consisten with theory. A further improvement would be to include polarization and neutrinos and see wether this has a noteworthy impact on our solutions.

REFERENCES

Baumann, D. 2020, Cosmology, Part III Mathematical Tripos, University of Cambridge. http://folk.uio.no/hansw/AST5220/notes/pdfs/baumann.pdf

Dodelson, S. 2003, Modern cosmology, San Diego, CA: Academic Press

Shen, S. 2019, AST4320: Cosmology and Extragalactic Astrophysics, Universitet i Oslo. https://www.dropbox.com/s/54oq0f97p3lvohl/AST4320Notes.pdf?dl=0

Tansem, H. 2020a, Milestone I: Computing the Hubble parameter and conformal time, Independent. https://github.com/hakontan/AST5220-Spring2020/blob/master/doc/milestoneI/milestone1.pdf

—. 2020b, Milestone II: Studying the recombination history of the universe., Independent. https://github.com/hakontan/AST5220-Spring2020/blob/master/doc/milestoneII/milestone2.pdf

Winther, H. A. 2020, Overview: Milestone III, Universitet i Oslo. http://folk.uio.no/hansw/AST5220/notes/milestone3.html